

# Effect of Annealing on the Structure and Properties of Polyvinylidene Fluoride Hollow Fiber by Melt-Spinning

Xianfeng Li, Xiaolong Lu

Key Laboratory of Hollow Fiber Membrane Materials and Membrane Process of Ministry of Education, Tianjin Polytechnic University, Tianjin 300160, China

Received 10 May 2006; accepted 31 July 2006

DOI 10.1002/app.25255

Published online in Wiley InterScience (www.interscience.wiley.com).

**ABSTRACT:** Polyvinylidene fluoride hollow fibers were prepared by melt-spinning technique under three spinning temperatures. The effects of annealing treatment on the structure and properties of hollow fiber were studied by differential scanning calorimetry (DSC), wide-angle X-ray diffraction (WAXD), tensile test, and scanning electron microscopy (SEM) measurements. DSC and WAXD results indicated that the annealing not only produced secondary crystallization but also perfected primary crystallization, and spinning and annealing temperature influenced the crystallinity of hollow fiber: the crystallinity decreased with the increase of spinning temperature; 140°C annealing increased the crystallinity, and hardly influenced the orientation of hollow fiber; above 150°C annealing increased the crystallinity as well, and furthermore

had a comparative effect on the orientation. The tensile tests showed that the annealed samples, which did not present the obvious yield point, exhibited characteristics of hard elasticity, and all the hollow fiber had no neck phenomenon. Compared with the annealed sample, the precursor presented a clear yield point. In addition, the annealed samples had a higher break strength and initial modulus by contrast with the precursor, and the 140°C annealed sample showed the smallest break elongation. SEM demonstrated the micro-fiber structure appeared in surface of drawn sample. © 2006 Wiley Periodicals, Inc. *J Appl Polym Sci* 103: 935–941, 2007

**Key words:** polyvinylidene fluoride; hollow fiber; melt-spinning; crystallization; property; annealing

## INTRODUCTION

Polyvinylidene fluoride (PVDF), as a partially fluorinated, semicrystalline polymer, can be used as an engineering material, electronic material, and coating and membrane material because of its outstanding mechanical properties, peculiar ferroelectric behavior, and good resistance to UV light and to many chemical environments, including acids, alkaline, strong oxidants, and halogens. So it has been an object of active scientific research for many years.<sup>1–3</sup>

Hollow fiber membrane is an important product of PVDF which has been widely used in industrial separation field, usually was prepared using the traditional solution phase inversion methods.<sup>2,3</sup> Compared with the phase inversion process, the melt-spinning process does not involve a large amount of organic solvent, should be emphasized. Recently

PVDF abrasive filament and fiber were prepared and studied<sup>4,5</sup> via melt-spinning technique. However, preparing PVDF membrane by melt-spinning are relatively poor, and Xu et al.<sup>6</sup> investigated the morphological textures of PVDF tubular films with five different molecular weights.

In fact, the melt-spinning and cold-stretching (MSCS) techniques have already been a standard process for preparing polypropylene (PP) and polyethylene (PE) microporous membranes, and preparation conditions have also been investigated.<sup>7–10</sup> In the melt-spinning process, a pure polymer is melt-spun, and the micropores are created by the mechanical force acting on the membranes in a subsequent cold-stretching step. Hence, in preparing porous membrane process by melt-spinning, there are three necessary steps: the first step is that a uniaxially oriented hollow fiber precursor with a stacked planar lamellar morphology is molten and extruded. The second step is to anneal this precursor. The third step is to uniaxially stretch the annealed precursor to form the final microporous membrane. Therefore, a crystal and oriented structure of hollow fiber is a very important prerequisite to prepare a significantly microporous material by this method.

The formation mechanism of membrane pore by MSCS has been proved to be related to the microcrystalline lamellae which are aligned in rows parallel to the extrusion direction. This structure can be

Correspondence to: X. Li (xianfengli@eyou.com).

Contract grant sponsor: Science Council of Tian Jin; contract grant numbers: 05YFJMJC04500, 05YFGDGX10000-1.

Contract grant sponsor: Ph.D. Programs Foundation of Ministry of Education of China; contract grant number: 20040058002.

Contract grant sponsor: Open Program of Key Laboratory of Hollow Fiber Membrane Materials and Membrane Process of Ministry of Education; contract grant number: 060518.

*Journal of Applied Polymer Science*, Vol. 103, 935–941 (2007)

© 2006 Wiley Periodicals, Inc.

obtained by high stress during the extrusion process and be improved by annealing. Micropore formation results from the lamellae spreading during the cold-stretching process. Therefore, the pore size and its distribution are dependent on structural properties such as crystallinity and degree of orientation of the hollow fiber before cold-stretching.

This article exhibits the effects of annealing time and temperature on structure and mechanical properties of PVDF hollow fiber to explore the technique of preparing PVDF hollow fiber membrane by MSCS process.

## EXPERIMENTAL

### Materials

Polyvinylidene fluoride (PVDF, solef1010, melting point 177°C) was supplied by Solvay (Tavaux, France).

### Preparation of hollow fiber

The hollow fiber precursors were prepared using a single-screw extruder (Melt Spinning Tester, Tokyo, Japan) with annular spinneret at the following conditions: The cooling air and water bath temperature was 24°C, the ratio of drawing about 15, and air gap length about 50 cm. Screw heater region I, II temperature, spinning, and take-up velocity were kept constant. The as-spinning hollow fiber precursors (PF-1, 2, and 3) are shown in Table I.

### Annealing treatment

The annealing treatment was performed in a heat oven. PF-1, 2, and 3 were annealed at 140, 150, and 160°C respectively, for 30 min, and the annealed hollow fiber samples (AF-4, 5, and 6) were obtained from the precursor sample PF-2, and AF-7, 8, and 9 from PF-3.

### Characterization of PVDF hollow fiber

#### Differential scanning calorimetry

About 10 mg hollow fiber samples were analyzed by differential scanning calorimetry (DSC) (Perkin-Elmer, DSC-7, Wellesley, MA) from room temperature to 200°C at 10°C/min heating rate. Crystallization heat  $\Delta H_c$  was determined from the exothermic peak area. The degree of crystallinity was evaluated by

$$\Phi_{\text{DSC}} = \Delta H_m / \Delta H_{100}$$

$\Delta H_{100} = 104.7$  J/g is the melting enthalpy for a 100% crystalline sample of PVDF.<sup>11</sup>

#### Wide-angle X-ray diffraction

The wide-angle X-ray diffraction (WAXD) patterns of the precursor and annealed samples were recorded by Bruker AXS D8 Discover with GADDS (Madison, WI). Cu K- $\alpha$  radiation ( $\lambda = 1.5418$  Å) was employed.

#### Scanning electron microscopy

The morphologies of drawn and undrawn hollow fiber samples were observed using a scanning electron microscopy (SEM, Quanta 200, Netherlands FEI).

#### Mechanical property measurements

The 250-mm-long fiber samples were tested at room temperature using an electronic single-yarn strength tester (PC-YG 061, Laizhou, China) on the basis of National Standard of China (GB/T 3916-1997), and the tensile rate was 250 mm/min. Then, the stress was calculated by pull force (N) and linear density of fiber (tex). For each specimen, no less than four runs were performed and representative sample property was exhibited. Break strength and initial modulus (MPa) came from the testing stress value (N/tex), and PVDF density was supposed as constant ( $\rho_{\text{PVDF}} = 1.78$  g/cm<sup>3</sup>).

## RESULTS AND DISCUSSION

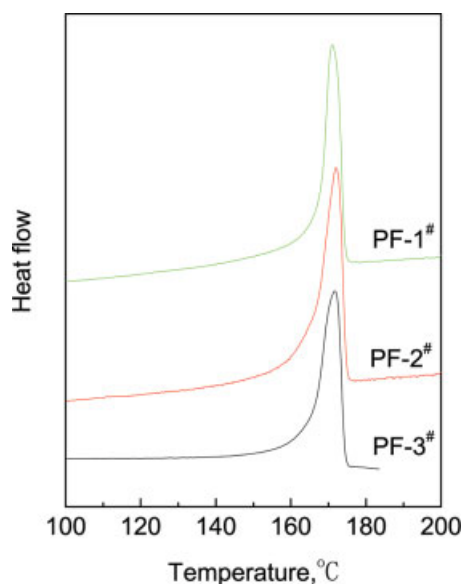
### DSC measurements

Figure 1 shows the effect of spinning temperature on DSC curves of PVDF hollow fiber. A similar, sharp melting peak presents at about 171°C, and crystallinity decreases slightly with the increase of spinning temperature. Theoretically, the viscosity of PVDF melt decreases when temperature increases, which leads to a lower spinline stress, and the draw-induced and shear-induced orientation in spinning fiber process are relaxed more easily. As a result, the higher spinning temperature influenced the orientation and crystallization property,<sup>12</sup> and the crystallinity became smaller when spinning temperature was higher.

From Figure 2, the effect of annealing and annealing temperature on DSC patterns of hollow fiber can be seen. Compared with the precursor, the annealed samples present a weak peak on the lower temperature side of the main peak. Furthermore, the temperature position of the weak peak approaches gradually to the main one (higher temperature) as the annealing temperature increases, while the temperature of the main peak practically does not change

TABLE I  
Preparation Conditions of Hollow Fiber Precursor

	PF-1	PF-2	PF-3
Spinneret heater temperature (°C)	230	250	270
Inner/outer radius (mm)	0.18/0.25	0.16/0.23	0.14/0.21



**Figure 1** Effect of spinning temperature on DSC curves of hollow fiber. [Color figure can be viewed in the online issue, which is available at [www.interscience.wiley.com](http://www.interscience.wiley.com).]

until the annealing temperature reaches 160°C adjacent to the main peak temperature (about 171°C). At that time it increases slightly.

Such DSC annealed-peaks of PVDF had been reported and their origins were summarized by Neidhöfer et al.<sup>13</sup> in their study in which, the secondary crystallization leading to the low endotherm evidenced by Marand and coworkers<sup>13-16</sup> was emphasized.

In their view,<sup>13-16</sup> secondary crystallization corresponds to the progressive formation of a population

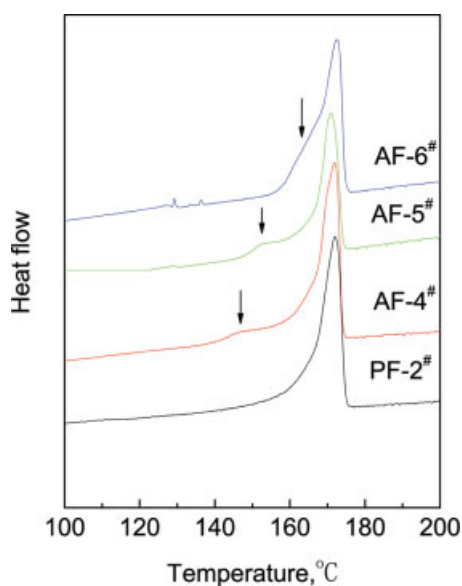


**Figure 2** DSC patterns of precursor sample and annealed samples at different temperature. [Color figure can be viewed in the online issue, which is available at [www.interscience.wiley.com](http://www.interscience.wiley.com).]

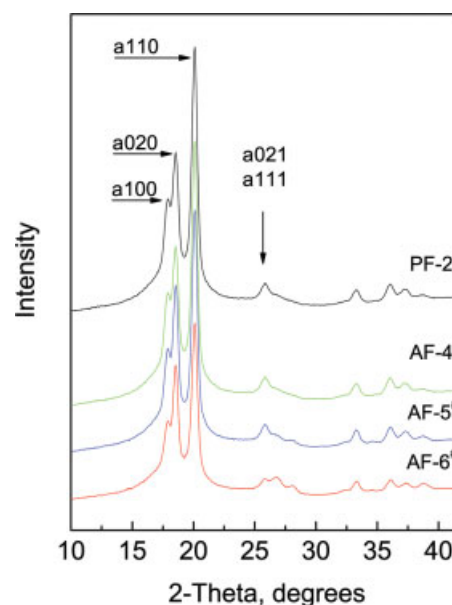


**Figure 3** WAXD patterns of precursor sample and annealed samples at different temperature. [Color figure can be viewed in the online issue, which is available at [www.interscience.wiley.com](http://www.interscience.wiley.com).]

of unstable crystals which melt at temperatures slightly above their formation temperature and much lower than the melting temperature of primary crystals. More definitely, secondary crystallization is a small cluster of chain segments of bundle-like or fringed-micellar structures. These chain segments originate from constrained amorphous regions in the vicinity of primary crystals. Via DSC, secondary crystals results in a low endotherm. This is opposed to the high endotherm which corresponds to melting of primary crystals, i.e., the usual lamellae structures which develops from an unconstrained melt.

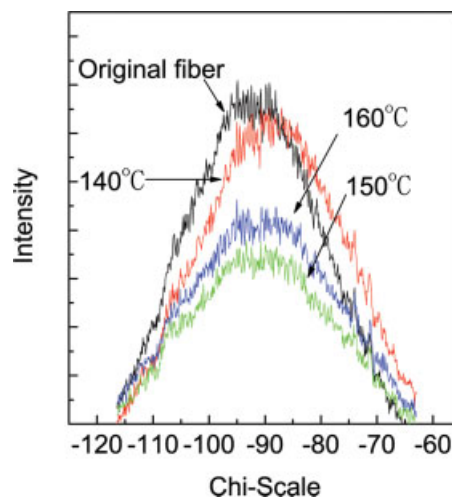


**Figure 4** Diffraction intensity evolution of sample crystallographic plane (002) at different annealing temperatures. [Color figure can be viewed in the online issue, which is available at [www.interscience.wiley.com](http://www.interscience.wiley.com).]

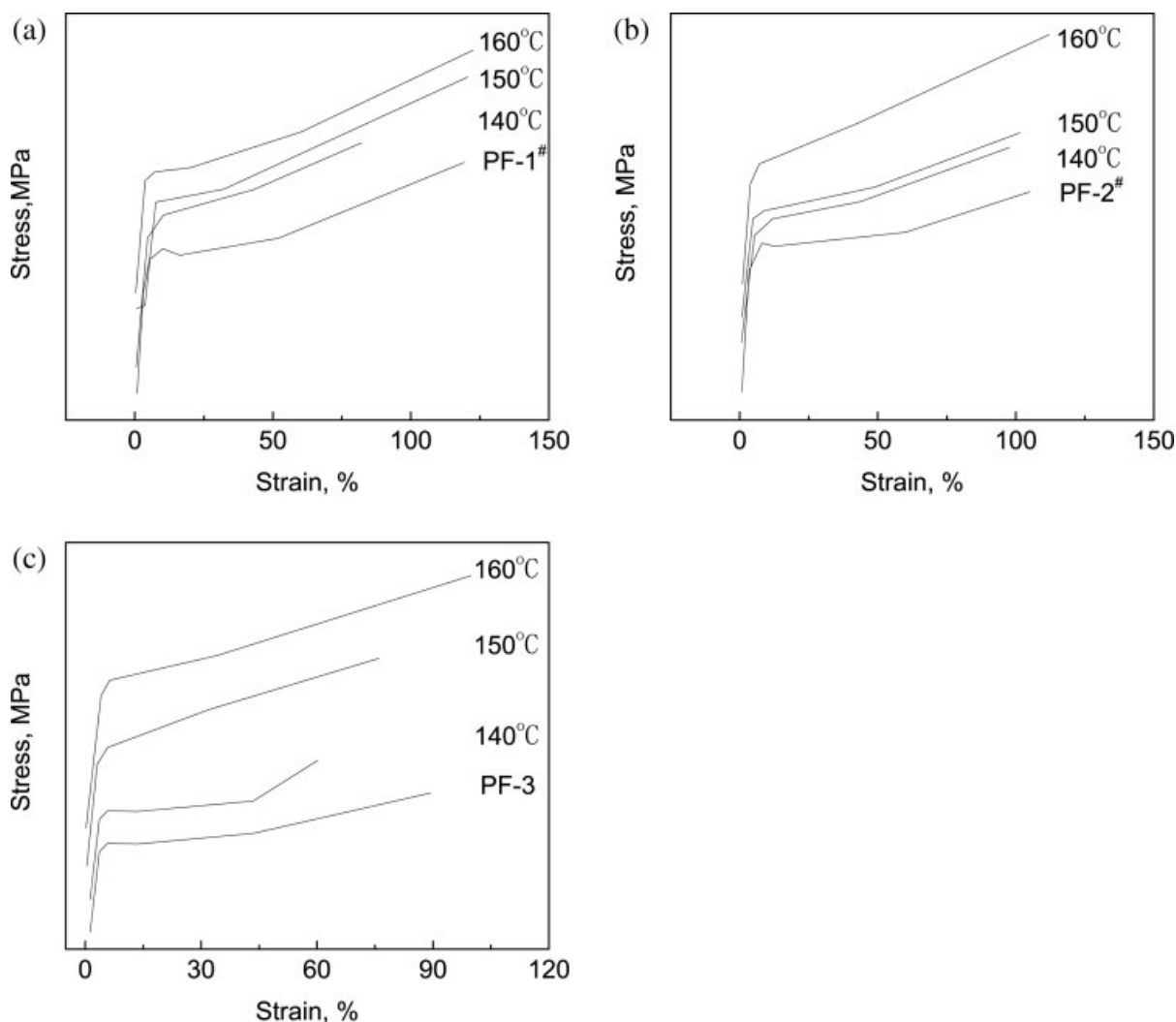


**Figure 5** Effect of annealing and annealing temperature on the curves of stress-strain (annealing time is 30 min).

It seems that the appearance and shift of the annealed-peak in this article can be explained properly on the basis of secondary crystallization. The trivial enhancement of the main melt peak of the 160°C annealed sample can perhaps be attributed to the more perfect crystals shown in WAXD test (Fig. 3).

Moreover, crystallinity of the entire annealed sample is higher than that of the precursor; however, the higher annealing temperature than 150°C reduced crystallinity by contrast to the 140°C annealing temperature. The most commonly known effects of annealing are the increases in crystallinity and crystalline size. These were confirmed by DSC and WAXD. But because the higher annealing temperature influenced the orientation frozen in hollow fiber (Fig. 4), it is tentatively presumed that some frozen orientation macromolecules could crystallize more easily at 140°C annealing; on the contrary, the frozen orientation macromolecules would be relaxed, and could not crystallize easily due to the higher anneal-

ing temperature. Then crystallinity reduces slightly as the annealing temperature increases.

In general, the annealing has two functions: perfecting the primary crystallization and leading to the secondary crystallization in the residual amorphous regions.

#### WAXD measurements

WAXD patterns (Fig. 3) show that the single peak at about  $2\theta = 27^\circ$  becomes a multi-peak as the annealing temperature increases which implies that the higher annealing temperature produced an obvious improvement of the resolution of the reflections at  $26.6^\circ$  and  $27.9^\circ$   $2\theta$  (021 and 111). This also suggests the increase of the crystallites dimensions towards the directions perpendicular to those crystallographic planes and the index of crystalline perfection,<sup>17</sup> while the first strong three reflections ( $17.6^\circ$ ,  $18.4^\circ$ , and  $19.9^\circ$   $2\theta$ ), which have the Miller index  $l = 0$  (100, 020, and 110) have no obvious change.

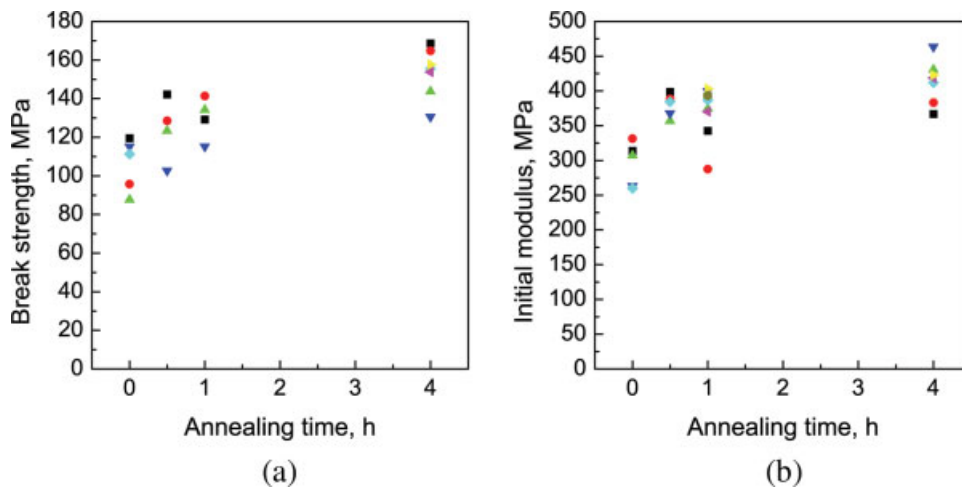


**Figure 6** Effects of the annealing time on the break strength and initial modulus of hollow fiber. The different symbols represent different tensile times. [Color figure can be viewed in the online issue, which is available at [www.interscience.wiley.com](http://www.interscience.wiley.com).]

WAXD patterns also show that no  $\beta$ -crystalline form in the precursors and annealed samples. In melt-spinning process,  $\beta$ -crystalline can be formed at a critical drawdown stress because of its polymorphic crystalline form.<sup>1</sup> But in this article, perhaps drawdown stress was too low to form  $\beta$ -crystalline. This was also indicated by DSC measurements.

The diffraction peak height of 002 crystallographic plane is used to qualitatively characterize the effect of annealing temperature on orientation of hollow fiber. As can be seen from Figure 4, 140°C annealing barely influences the orientation of hollow fiber, while the orientation decreases slightly, as annealing temperature increases.

### Characterization of mechanical property

Effect of annealing temperature on the curves of stress–strain

The tensile tests show that neither the precursor nor the annealed sample showed neck phenomenon. How-

ever, from the stress–strain curves (Fig. 5), it can be seen that all the three kinds of precursors present a yielding point clearly, and the yielding point of the annealed sample becomes unambiguous, even the yielding point almost disappears with the increase of annealing temperature, which indicates that annealed PVDF hollow fiber has the characteristics of hard elasticity. This result was also reported in literature.<sup>5</sup>

The repetitious tensile tests present a general trend that the break elongation of the 140°C annealed sample is the smallest among the precursor and the annealed sample. By comparing the precursor sample with the aforementioned 150°C annealed samples, it was found that the break elongation does not have a systematical trend. The crystallization and orientation can be used for explaining the result. When annealing at 140°C, the crystallinity increased, and the orientation hardly changed, as a result, the break elongation decreased. But annealing at above 150°C, the orientation was also influenced although

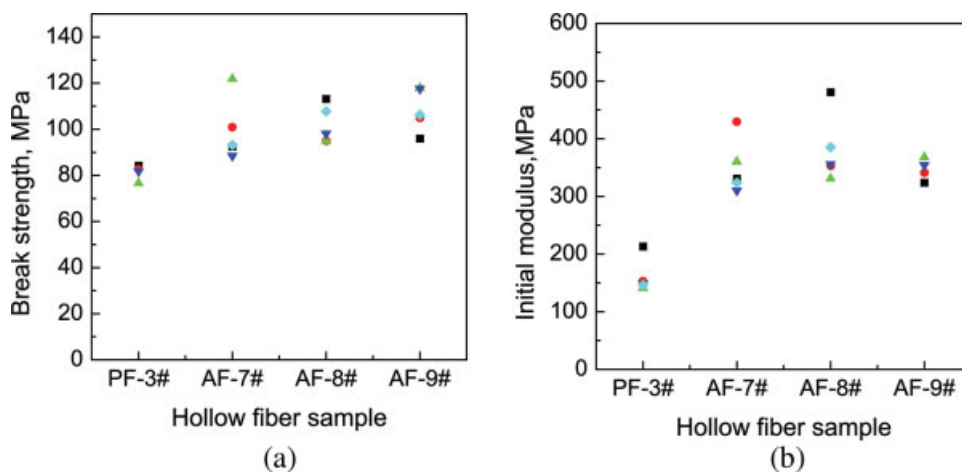


**Figure 7** Effect of the annealing temperature on the break strength and initial modulus of hollow fiber. The different symbols represent different tensile times. [Color figure can be viewed in the online issue, which is available at [www.interscience.wiley.com](http://www.interscience.wiley.com).]

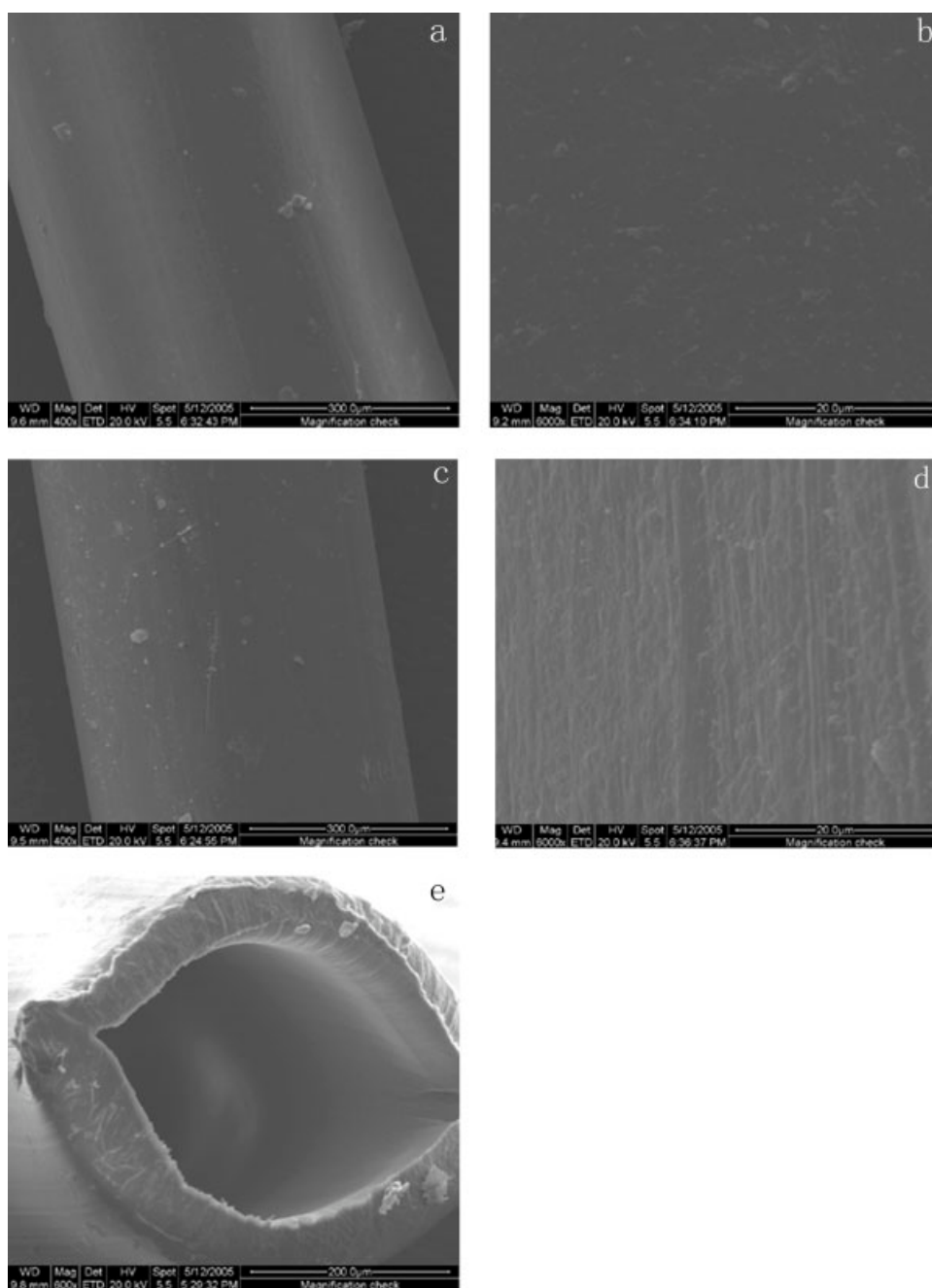


**Figure 8** Surface and cross section morphologies of undrawn and drawn hollow fiber. (a, b) undrawn surface; (c, d) drawn surface; and (e) cross section.

crystallinity increased, so the break elongation was influenced by two factors, and then no obvious trend was observed.

#### Effect of annealing time and temperature on break strength and initial modulus

The effects of the annealing time on break strength and initial modulus are shown in Figure 6. The annealing treatment enhances obviously break strength and initial modulus of hollow fiber. When annealing time is less

than 1 h, initial modulus increase sharply, and after 1 h, the enhancement trend of initial modulus becomes flat.

The effects of annealing temperature on break strength and initial modulus are shown in Figure 7. It can be seen that the 140°C annealing has a strong influence on break strength and initial modulus, while much higher annealing temperature than 140°C did not produce remarkable influence compared with the 140°C annealed sample. In addition, the effect of annealing on the initial modulus is stronger than on the break strength.

The enhancement of break strength and initial modulus can attribute to evolution of hollow fiber structure: the increase of crystallinity and comparative change of orientation, which had been demonstrated by DSC and WAXD.

### Characterization of morphology

Figure 8 indicates, in contrast with undrawn hollow fiber, that drawn hollow fiber presents a clear microfibrillar structure characteristic, but no micropore appeared in the drawn hollow fiber. The SEM of drawn samples was obtained at a 250 mm/min drawing rate. For preventing the recovery of drawn-fiber, the length of fiber was fixed after the hollow fiber was drawn, and the annealing was performed at 140°C for about 5 min. The flat cross section sample was obtained by cutting hollow fiber because fracturing hollow fiber in liquid nitrogen tended to rupturing along the microfibrillar direction.

### CONCLUSIONS

Spinning temperature influenced the crystallinity of hollow fiber that decreased with the increase of temperature. The effect of the annealing treatment on the crystallization presented at two aspects: one was to perfect the primary crystallization; another was to result in the secondary crystallization, and then the crystallinity increased when the precursors were annealed. Furthermore 140°C annealing hardly influenced the orientation of hollow fiber, the above 150°C annealing influenced comparatively the orientation. The tensile tests showed that the annealed sample exhibited obviously characteristics of hard elasticity fiber, did not present the yield point, and

all the hollow fiber (including the precursor and the annealed sample) had no neck phenomenon. However, the precursor presented a clear yield point by contrast with the annealed sample. Moreover, the annealed sample had a higher break strength and initial modulus in comparison with the precursor, and the break elongation of the 140°C annealed sample was the smallest. SEM demonstrated that the drawn sample presented a microfibrillar structure.

### References

1. Wang, Y.; Cakmak, M.; White, J. L. *J Appl Polym Sci* 1985, 30, 2615.
2. Lin, D. J.; Chang, C. L.; Chen, T.-C.; Cheng, L.-P. *Desalination* 2002, 145, 25.
3. Lin, D. J.; Chang, C. L.; Huang, F. M.; Cheng, L. P. *Polymer* 2003, 44, 413.
4. Susa, T.; Ohira, S.; Endo, H. U.S. Pat. 5,288,554 (1994).
5. Du, C.; Zhu, B.; Xu, Y. *J Mater Sci* 2005, 40, 1035.
6. Xu, J.; Johnson, M.; Wilkes, G. L. *Polymer* 2004, 45, 5327.
7. Kim, J. J.; Jang, T. S.; Kwon, Y. D.; Kim, U. Y.; Kim, S. S. *J Membr Sci* 1994, 93, 209.
8. Li, J.-M.; Xu, Z.-K.; Liu, Z.-M.; Yuan, W.-F.; Xiang, H.; Wang, S.-Y.; Xu, Y.-Y. *Desalination* 2003, 155, 153.
9. Johnson, M. B.; Wilkes, G. L. *J. Appl Polym Sci* 2002, 84, 1076.
10. Yu, T.; Wilkes, G. L. *Polymer* 1996, 37, 4675.
11. Rosenberg, Y.; Sigmann, A.; Narkis, M.; Shkolnik, S. *J Appl Polym Sci* 1991, 43, 535.
12. Foreman, J. A.; Klinger, K. A.; Wolkowicz, M. *Thermochim Acta* 1996, 272, 147.
13. Neidhöfer, M.; Beaume, F.; Ibos, L.; Bernès, A.; Lacabanne, C. *Polymer* 2004, 45, 1679.
14. Alizadeh, A.; Richardson, L.; Xu, J.; McCartney, S.; Marand, H.; Cheung, Y. W.; Chum, S. *Macromolecules* 1999, 32, 6221.
15. Marand, H.; Alizadeh, A.; Farmer, R.; Desai, R.; Velikov, V. *Macromolecules* 2000, 33, 3392.
16. Alizadeh, A.; Sohn, S.; Quinn, J.; Marand, H.; Shank, L. C.; Darrell Iler, H. *Macromolecules* 2001, 34, 4066.
17. Marega, C.; Marigo, A. *Eur Polym J* 2003, 39, 1713.